Epidermal stem cell-derived exosomes alleviate autophagy induced endothelial cell apoptosis through miR200b-3p/ERK pathway in diabetic wounds

hailin Xu
Sun Yat-sen University First Affiliated Hospital
Zhiyong Wang
Sun Yat-sen University First Affiliated Hospital
Hao Yang
Sun Yat-sen University First Affiliated Hospital
Chufen Chen
Sun Yat-sen University First Affiliated Hospital
Yunxian Dong
Sun Yat-sen University First Affiliated Hospital
Zhongye Xu
Sun Yat-sen University First Affiliated Hospital
Dongming Lv
Sun Yat-sen University First Affiliated Hospital
Peng Wang
Sun Yat-sen University First Affiliated Hospital
Mingzhou Yuan
Sun Yat-sen University First Affiliated Hospital
Xiaoyan Wang
Sun Yat-sen University First Affiliated Hospital
Miao Chen
Sun Yat-sen University Cancer Center
Bing Tang
Sun Yat-sen University First Affiliated Hospital
Zhicheng Hu
Sun Yat-sen University First Affiliated Hospital
Wuguo Deng
Sun Yat-sen University Cancer Center
Jiayuan Zhu (zhujiay@mail.sysu.edu.cn)
The First Affiliated Hospital of Sun Yat-sen University https://orcid.org/0000-0003-1501-6999

Research Article

Keywords: diabetes, diabetic wound, exosomes, stem cell, apoptosis, endothelial cell

Posted Date: June 16th, 2022

DOI: https://doi.org/10.21203/rs.3.rs-1734539/v1

Abstract

Backgrounds: Diabetic wounds have the characteristics of abnormal inflammatory response, decreased neovascularization, and disturbed microenvironment. Clinical use of epidermal basal cell suspensions promotes chronic wound healing. Further study found that rat Epidermal stem cells (EpiSCs) could promote the angiogenesis of full-thickness wounds in SD rats. The mechanism of the effect of EpiSCs on wound healing warrants further study.

Methods: In vivo, EpiSCs were labeled with enhanced green fluorescent protein and then sprayed on dorsal wound of db/db mice. The quality of wound healing was estimated by the residual wound area rate and Hematoxylin and Eosin (H&E) staining. Expression of neovascular markers and collagen formation were elucidated by immunohistochemistry (IHC), immunofluorescence (IF), and MASSOM.

In vitro, the supernatant of EpiSCs were ultra-centrifugated to collected exosomes (EpiSC-EXOs). Human umbilical vein endothelial cells (HUVECs) were treated with high glucose and EpiSC-EXOs. miR 200b-3p is identified abundant in EpiSC-EXOs using RNA sequencing. HUVECs were analyzed with apoptosis rate, ROS level, proliferation and mitochondrial membrane potential.

Results: In vivo, Epidermal stem cells (EpiSCs) could colonize in wounds, promoting angiogenesis thus accelerating wound healing in diabetic mouse model (db/db mouse). In vitro, EpiSC-EXOs had the ability to reduce apoptosis by downregulating excessive autophagy induced by high-glucose conditions. Furthermore, we found that miR200b-3p rich in EpiSC-EXOs affected the phosphorylation of ERK by targeting SYDE1 to regulate intracellular autophagy levels, thereby reducing vascular endothelial cell apoptosis caused by a high-glucose environment.

Conclusions: Collectively, our results verified the effect of EpiSC-EXOs on apoptosis caused by a high-glucose environment in vascular endothelial cells and revealed that its underlying mechanism occurs through the miR200b-3p/SYDE1/RAS/ERK pathway. Our study explains the role of EpiSCs in promoting wound healing in diabetic patients.

Background

Chronic wounds constitute a type of age-related disease, and one of its leading causes is diabetic mellitus (DM)(1). Currently, the standard treatments for diabetic wounds are debridement, negative pressure aspiration, and skin grafting(2, 3). However, due to the characteristics of diabetic wounds, such as an abnormal inflammatory response, decreased angiogenesis, and disturbance of the microenvironment of the wound surface, these treatments have achieved limited benefits(4). As wound healing is a heavy burden for patients both physically and financially, how to rebalance microenvironments and provide better conditions for wound healing remain major challenges in clinical treatment(1).

In general, the wound healing process can be divided into several stages: immediate hemostasis, acute inflammation, proliferation, and maturation(5). In normal wounds, injured tissue proliferates rapidly in granulation tissue, characterized by intense angiogenesis(6). The most important feature of diabetic wounds is the decrease in the number of new blood vessels in the wound, resulting in insufficient blood supply to the wound, which in turn affects cell proliferation and tissue restructuring(7). One of the purposes of clinical treatment is to provide a sufficient blood supply to the wound to promote the proliferation of wound cells and the survival of skin grafting(8, 9). Therefore, how to further improve the number of blood vessels on the wound is important to the healing of diabetic ulcers.

Stem cell-based therapy is considered a promising approach for treating diabetic wounds because stem cells are pluripotent, can self-renew and have the ability to regulate their microenvironment(10). Our previous study found that epidermal basal cell suspensions, which contain epidermal stem cells (EpiSCs), can promote wound healing in patients with or without diabetes(11, 12). Additional studies found that EpiSCs can proliferate in the wound area and accelerate wound healing in SD rats and DB/DB mice(13, 14). EpiSCs have the ability to promote angiogenesis and regulate inflammation in chronic wounds(13). However, how EpiSCs affect these biological processes and promote wound healing remains unknown.

Exosomes, with a diameter of approximately 100 nm, are among of the components secreted by almost every cell(15). The uptake and release of exosomes is an important means to communicate information between cells over long distances(16). Studies have found that exosomes from different kinds of stem cells can regulate wound healing(17–19). The role of exosomes in the diagnosis and treatment of clinical diseases has been gradually revealed(20). It is believed that these extracellular vesicles, which are rich in proteins, lipids and nucleic acids, are the main contributors to stem cell efficacy.

MicroRNAs (miRNAs), which are short (19- to 25-nt) RNAs, are one of the main substances that are abundant in exosomes(21). MicroRNAs target the 3' untranslated region of mRNAs, forming a transient double-stranded miRNA duplex, and then the mature miRNA strand is incorporated into the RNA-induced silencing complex to mediate gene silencing and passenger strand degradation(22). A single miRNA can target hundreds of mRNAs and influence the expression of many genes(23). Moreover, miRNAs delivered by exosomes function as posttranscriptional regulators by forming silencing complexes that further affect biological processes within cells(24).

Apoptosis and autophagy are important intracellular processes that maintain organism homeostasis and promote survival(25). Autophagy involves the selective degradation of damaged cellular organelles and protein aggregates, while apoptosis involves the removal of damaged or aged cells(26, 27). Apoptosis and autophagy are in a state of dynamic equilibrium within the cell(28). Autophagy is induced when there is proper external stimulation, thereby coping with organelle damage, such as endoplasmic reticulum stress, to promote cell survival(29). Excessive external stimulation unsuitable for cell survival, such as a high-glucose environment, can lead to the induction of excessive autophagy, which further leads to autophagy-induced apoptosis(30–32). In our study, we found that excessive autophagy is the reason for endothelial cell apoptosis under high-glucose conditions. Therefore, the inhibition of excessive autophagy

within cells under extreme conditions promotes cell survival and further benefits the healing process of diabetic wounds.

In our study, we found that miR200b-3p delivered by epidermal stem cell-derived exosomes (EpiSC-EXOs) downregulated high glucose-induced endothelial cell apoptosis, which further explained the effectiveness of EpiSCs in diabetic wound healing.

Material And Methods

Cells and cell culture

Six-day-old mice were sacrificed by cervical dislocation. Human foreskin was collected at the First Affiliated Hospital of Sun Yat-sen University. Animal ethics approval was obtained from the First Affiliated Hospital of Sun Yat-sen University of Animal Ethics Committee. Informed consent has been obtained from patients when appropriate. The skin was removed and placed in a 15-ml centrifuge tube that contained 1% phosphate-buffered saline (PBS; 10010023; Gibco) and placed on ice. The subcutaneous fascia was removed, and the skin was cut to a size of 1 cm × 1 cm and then digested in MYSEED follow the instruction at 37°C for 30 min so that the epidermis could be scraped off using a sterile scalpel. The epidermis was then collected and digested in 0.25% trypsin-EDTA solution for 5 min. T25 culture flasks were pre-coated with 1 ml (0.5 mg/ml) of fibronectin (FN; ~5 μg/cm^2; Shanghai Fibronectin Biotechnology, Shanghai, China) solution. Next, the digested cell suspension was filtered in a 50-ml centrifuge tube using a 200-mesh filter and centrifuged at 1000 r/min for 10 min. The pellet was resuspended in 4 ml of keratinocyte serum-free medium (K-SFM; 17005042; Gibco). The basal cell suspension was then used to coat the culture flask and incubated at 37°C for 20 min. Approximately 10% of the cells regarded as EpiSCs adhered to the wall first. EpiSCs were cultured in K-SFM media at 37°C, and the medium was changed every 2 days.

Human umbilical vein endothelial cells (HUVECs) were purchased from ScienCell (#8000, ScienCell). The cells were cultured in endothelial cell medium (ECM, #1001, ScienCell) in a humidified incubator with 5% carbon dioxide added, and the medium was changed every 2 days. For experimental treatment, HUVECs at p4 were subjected to normal glucose (NG, 5 mmol/L) or high glucose (HG, 30 mmol/L) for further experiments.

Fluorescence microscopy

Cells or tissue samples were washed 3 times with PBS for 5 min each, fixed with 4% paraformaldehyde (P0099; Beyotime Biotechnology) for 20 min, washed again with PBS 3 times, and then incubated with 0.5% Triton X-100 (P0096; Beyotime Biotechnology) at room temperature for 20 min. The samples were washed with PBS three times and then incubated with 5% goat serum (SL038; Solarbio) blocking solution at room temperature for 40 min. Next, the cells were incubated with ITGα6 (1:200; ab181551; Abcam), k15 (1:200; ab52816; Abcam), Ki67 (1:200; ab15580; Abcam), and CD31 (1:200; ab24590; Abcam) antibodies at 4°C overnight. Then, the cells were incubated with Cy3-conjugated AffiniPure goat anti-mouse/rabbit

IgG (H + L) (SA00009-1/SA00009-2; Proteintech) or CoraLite 488-conjugated goat anti-mouse/rabbit IgG (H + L) (SA00013-1/SA00013-2; Proteintech), which are secondary antibodies, at room temperature for 60 min. DAPI (C0065; Solarbio) was used for nuclear counterstaining. Then, the samples were washed 3 times with PBS for 5 min each. The supernatant was aspirated, after which the samples were mounted with an anti-fluorescence quencher and observed under a fluorescence microscope.

Tube formation assays

Matrigel Matrix (356234, Corning) was plated in 48-well culture plates and then incubated at 37°C for 20 min. HUVECs were cultured on Matrigel with different glucose concentrations or other components. After incubation at 37°C for 4 h, tube formation was assessed under a microscope and analyzed by measuring the tube branches.

HUVEC cotransfection for functional assays

HUVECs at p4 were transiently transfected with miR200b-3p mimic/miR200b-3p inhibitor/NC sequence (Ribobio) using Lipofectamine® 3000 (L3000015-1.5ML; Thermo Fisher) according to the manufacturer's instructions. Two days after transfection, the cells were treated with different glucose concentrations or other treatments for further experiments.

Flow cytometry

Cell identification

EpiSCs were collected by centrifugation. The cells were then resuspended in 0.1 ml of PBS with K10 (1:50; NBP2-61736, Novus) or ITGα6 (1:50; ab181551; Abcam) for 30 min. Then, the cells were collected and stained with CoraLite594-conjugated goat anti-mouse IgG (H + L) (SA00013-3; Proteintech) on ice and protected from light for 30 min. Afterward, the cells were rinsed in 0.5 ml of PBS and subjected to flow cytometry analysis.

Annexin-V/PI staining

Apoptosis was measured by flow cytometry. HUVECs at p4 were collected by centrifugation, followed by two rounds of cell pellet washing with PBS. After resuspension with binding buffer, the cells were stained with 10 μl of Annexin V-fluorescein isothiocyanate (FITC) and 5 μl of propidium iodide (PI) for 10 min in the dark. The stained cells were subsequently analyzed by flow cytometry.

Detection of ROS

Cells were pretreated with high glucose and other treatment components, rinsed and then washed with cold PBS, after which they were incubated with 1 mM DCHF-DA in the dark at 37°C for 20 min. The cells were then trypsinized, washed with PBS again and resuspended in PBS. The stained cells were analyzed by flow cytometry.

CCK-8 assays

Cell viability was detected by a CCK-8 assay according to the manufacturer's instructions (Dojindo Molecular Technologies, Rockville, USA). HUVECs were seeded into 96-well plates at a density of 4500 cells/well. The cells were subjected to a high glucose concentration for 24/48/72 h. Then, 10 μM CCK-8 was added to each well for 2 h of incubation. The absorbance at 450 nm (OD450) was measured using an enzyme labeling apparatus.

Mitochondrial membrane potential (ΔΨm)

JC-1 (5,5',6,6'-tetrachloro-1,1',3,3'-tetraethylbenzimidazolcarbocyanine iodide) (HY-15534; MCE), a lipophilic cationic dye that can selectively enter mitochondria, was used for visualization. HUVECs were seeded into 6-well plates and subjected to a high concentration of glucose and other treatment components. JC-1 (final concentration of 2 μM) was applied to the cells, which were then incubated at 37°C under 5% CO2 for 15–20 min and assessed via fluorescence microscopy.

RNA extraction and real-time PCR analysis

Total RNA was extracted from HUVECs using an RNA purification kit (R4013-03, Magen) following the manufacturer’s instructions. Total RNA was reverse transcribed using a HiScript-TS 5/3’ RACE Kit (RA101-01; Vazyme). Real-time qPCR was performed using ChamQ SYBR Color qPCR Master Mix (Q421-02; Vazyme). The data were obtained as cycle threshold (Ct) values, and the 2 − ΔCt method was used for the analysis.

Luciferase activity assays

We constructed wild-type and mutated SYDE1 3'-UTR luciferase reporter plasmids with the potential binding site of miR200b-3p and transfected them with miR200b-3p mimics or miR-NC into HUVECs. Rinella luciferase was used as an internal control. The luciferase activities were measured by a Dual-Luciferase Reporter Assay System (E1910; Promega). The luciferase activity assays were conducted following the manufacturer’s instructions.

Western blots

For Western blot analysis, HUVECs were lysed in RIPA buffer (FD009, Fdbio Science) with 1% protease and 1% phosphatase inhibitors (A8260; Solarbio). The protein content was determined using the Bradford assay (Sigma–Aldrich), and 50 μg of lysates was separated by electrophoresis using 4–12% polyacrylamide gel electrophoresis (PAGE) gels and transferred onto a PVDF membrane (IPVH00010; Millipore). After membranes were blocked with 5% nonfat dried milk, they were incubated with the following primary antibodies overnight at 4°C: SYDE1 (1:2000; NBP1-57607; Novus), P-RHOA (1:2000; 9968T; CST), ROHA (1:2000; 9968T; CST), P-ERK (1:2000; #4370; CST), P-38 (1:2000; #8690; CST), LC3 (1:2000; PD014; MBL), and GAPDH (1:5000; 10494-1-AP; Proteintech). Afterward, the membranes were incubated with appropriate secondary IgG antibodies at a 1:10000 dilution for 1 h at room temperature. Protein-antibody complexes were then detected by chemiluminescence (Pierce ECL Western blotting Substrate, Thermo, USA).

Animal experiment

Twenty mouse were anesthetized by inhaling isoflurane (INH), and a 8mm diameter, full-thickness wound was made on the dorsal skin of each mouse. The wounds were randomly divided into different groups. To explore the function of ESCs in diabetic wounds in vivo, 0.5 ml of EpiSCs stably expressed EGFP at a density of 2×10^5/ml was eve were evenly sprayed on the wound bed using a 2-ml syringe. For the control group, 1 ml of PBS was sprayed. To explore the function of miR 200b-3p in diabetic wounds in vivo, agomiR 200b-3p or NC were injected to the subcutaneous at the dose of 60nmol/Kg. The wound healing time was recorded, and the residual wound area rate was calculated as [(day n area)/(day 0 area)] × 100% (n = 0, 3, 7, 10 or 14). Five rats of each group were sacrificed on days 0, 3, 7, 10 and 14, respectively, and the wound tissues were harvested and separated into two halves across the center: one half was processed for histological and immunohistochemistry analyses, and the other was rapidly frozen in liquid nitrogen for immunofluorescence.

Statistical analysis

The results are expressed as the means ± SEMs, unless otherwise indicated. Differences between groups were evaluated using one-way ANOVA. All reported p values were two-sided. A p value of < 0.05 was considered statistically significant. Statistical analyses were performed using SPSS 20.0 software (SPSS, Chicago, IL, USA) and GraphPad Prism 8.0.

Results

EpiSCs accelerate wound healing by promoting angiogenesis

To study the effective substance in epidermal basal cell suspensions that promote chronic wound healing in patients with diabetes mellitus, we first collected EpiSCs from human foreskin and newborn mouse skin and then cultured the harvested EpiSCs in K-SFM medium. The EpiSCs obtained were morphologically uniform, elliptical in shape and had large nuclei (Fig. 1A). The EpiSCs were verified by immunofluorescence microscopy, which showed high expression of the basement membrane-related marker ITGα6 and EpiSC-related labels K15 and Ki67 (Fig. 1B) and low expression of the keratinocyte terminal differentiation marker K10, and their purity reached 96% (Fig. 1C).

Next, EpiSCs were labeled with green fluorescence using EGFP lentivirus (Fig. 2A) and applied to the dorsal wound model in db/db mice. The dorsal wound using EpiSCs healed completely within 2 weeks and had a better healing quality, while the control group still had some unhealed wounds remaining (Fig. 2C, Fig. S1A-E). The wounded tissue was taken 7 days after surgery, and we found that EpiSCs with green fluorescence colonized and survived in the wound bed (Fig. 2B). We also found that the angiogenesis in wound beds of the EpiSC groups was significantly higher than that of the control group (Fig. 2D), which suggested that EpiSCs accelerated wound healing by promoting angiogenesis in DB/DB mice.

High glucose induces endothelial cell malfunction, and EpiSC-EXOs alleviate apoptosis in HUVECs

To explore the role of EpiSCs sprayed on the wound surface in the process of diabetic wound healing, we used high-glucose medium for culturing HUVECs to mimic diabetic conditions in vitro. The results showed that the proliferation rate and tube formation ability of HUVECs decreased under high-glucose conditions (Fig. 3A-B). We then screened for differences in the transcription level between HUVECs under high-glucose (30 mmol/L, HG) and normal glucose (5 mmol/L, NG) conditions by transcriptome sequencing (Fig. 3C). The differentially expressed genes were analyzed for Kyoto Encyclopedia of Genes and Genomes (KEGG) pathway enrichment (Fig. 3D), which showed that these genes were mainly enriched in apoptosis and oxidative phosphorylation (Fig. 3E). Therefore, we assumed that a high-glucose environment could enhance the production of reactive oxygen species (ROS) within cells and promote apoptosis (Fig. 3G). This supposition was confirmed by elevated ROS detected by DCFH-DA (Fig. 3F).

Considering that EpiSCs sprayed onto the wound surface promoted angiogenesis in db/db mice and that exosomes have been reported to be the main contributor to stem cell efficacy(19), we investigated whether EpiSC-EXOs alleviate apoptosis in HUVECs under high-glucose conditions. EpiSC supernatant was collected and ultracentrifuged to harvest EpiSC-EXOs, which were verified by nanoparticle tracking analysis (NTA), electron microscopy, and Western blotting (Fig. 4A-D). Subsequently, EpiSC-EXOs were added to high glucose-treated HUVECs at a concentration of 50 μg/ml. We found that EpiSC-EXOs significantly reduced apoptosis induced by high-glucose conditions in HUVECs (Fig. 4E).

Excessive autophagy is the main cause of apoptosis

To test whether lowering the ROS level is sufficient to suppress apoptosis of HUVECs in a high-glucose environment, we treated HUVECs under high-glucose conditions with N-acetyl-L-cysteine (NAC), a reactive oxygen scavenger. Surprisingly, although NAC indeed decreased the ROS level in HUVECs under high-glucose conditions, it did not affect the apoptosis rate of HUVECs (Fig. 5A, E). Therefore, we assume that maybe the upregulation of ROS is just an outcome of several intracellular prosses that leads to apoptosis, thus simply eliminating ROS is not sufficient to inhibit apoptosis induced by high-glucose conditions.

Many forms of intracellular stress may lead to cell apoptosis, including endoplasmic reticulum stress, metabolic pressure, and mitochondrial damage. We found the upregulation of ER stress related genes (Fig. S3B), as well as decreased intracellular mitochondrial membrane potentials indicated by JC1 in HUVECs under high-glucose condition (Fig. 5B). To deal with intracellular stress, cells usually increase their autophagy level to remove damaged organelles and ROS in cells. A mRFP-eGFP-LC3 plasmid is used to show that autophagy is up regulated in HUVECs under high-glucose conditions, and this increase in autophagosomes is related to increased autophagic flux not to the block of the autophagosomes-lysosomal fusion (Fig. 5C). The up regulation of autophagy is also observed in patients with diabetic

ulcers (Fig. S2). Rapamycin, an autophagy agonist, significantly reduced the level of ROS but induced apoptosis of HUVECs under high-glucose conditions. In contrast, chloroquine, an inhibitor of autophagy, significantly reduced the apoptosis rate (Fig. 5D, F).

miR200b-3p, enriched in EpiSC-EXOs, suppresses apoptosis of HUVECs in a high-glucose environment

As mentioned above, we found that exosomes derived from EpiSCs significantly reduced the apoptosis rate of HUVECs in a high-glucose environment. To further study the mechanism contributing to the effectiveness of EpiSC-EXOs, we identified 44 upregulated and 32 downregulated miRNAs by comparing the sequencing results between fibroblast-derived exosomes (Fb-EXOs) and EpiSC-EXOs (Fig. 6A-C). Among the top 5 upregulated miRNAs, miR200b-3p dramatically decreased the apoptosis rate of HUVECs under high-glucose conditions (Fig. 6D). Consistently, mitochondrial membrane potential was restored and ROS production was decreased in HUVECs overexpressing miR200b-3p (Fig. 6E-F). Therefore, miR200b-3p is a key component in EpiSC-EXOs that inhibits apoptosis of HUVECs in high-glucose environments.

miR200b-3p regulates autophagy through the SYDE1/RAS/ERK pathway.

To explore how miR200b-3p affects the apoptosis of HUVECs in a high-glucose environment. Transcriptome sequencing was performed and revealed that the differentially expressed genes were mainly enriched in the MAPK pathway (Fig. 7A-B), which was consistent with the results of the enrichment analysis of miR200b-3p targets predicted from the online database (Fig. 7D). To identify the specific target genes of miR200b-3p, we selected the common differentially expressed genes among the pools of HG vs. NG, miR200b-3p up vs. miR200b-3p down, and miR200b-3p predicted targets (Fig. 7C). RT–qPCR was performed to validate the change in the expression of these 7 candidate genes in high-glucose-treated cells with miR200b-3p overexpression and knockdown. We found that SYDE1 had the lowest expression in miR200b-3p-overexpressing cells (Fig. 7E).

Synapse Defective Rho GTPase Homolog 1 (SYDE1) encodes a RhoGAP that negatively regulates phosphorylation of RAS family proteins such as RHOA(33). RAS is an upstream player of the MAPK pathway that regulates the phosphorylation of ERK, which could negatively regulate autophagy. In line with our previous sequencing results and hypothesis, SYDE1 was confirmed to be a target of miR200b-3p via a dual-luciferase reporter system (Fig. 7F). Silencing of SYDE1 by miR200b-3p promoted the phosphorylation of ERK and further suppressed autophagy in HUVECs in a high-glucose environment (Fig. S3A). Western blotting of SYDE1, p-ERK and LC3 was performed to demonstrate the decreased autophagy level caused by miR200b-3p (Fig. 7G). In conclusion, miR200b-3p inhibits excessive autophagy of cells under high-glucose conditions through the SYDE1/RAS/ERK pathway, thereby reducing the apoptosis rate of HUVECs.

miR200b-3p promotes neovascularization and wound healing in diabetic mice

To examine whether miR200b-3p has the same effects in vivo, we used a dorsal wound model of db/db mice with a diabetic background. Two circular wounds of approximately 8 mm in diameter were created, and then agomiR200b-3p or NC was administered (Fig. 8A). The wound area sections on day 7 were stained with CD31 for immunohistochemical analysis. As shown in Fig. 8, the agomiR200b-3p group had a smaller residual wound area, higher healing quality, shorter healing time and more neovascularization (Fig. 8A-D, Fig. S4A-C). These results suggested that miR200b-3p could promote neovascularization and improve wound healing in db/db mice.

Discussion

Persistent hyperglycemia is the most important feature of diabetes, which can lead to organ dysfunction such as that associated with diabetic vasculopathy. The malfunction of vascular endothelial cells mainly manifested as arteriosclerosis occlusion and vascular lumen narrowing. These blood supply capacity disorders and decreased neovascularization further lead to the lack of healing of diabetic ulcers. Therefore, it remains a major challenge to improve blood supply to the wound bed in the clinical treatment of diabetic ulcers. In our study, we found EpiSCs could improve diabetic wound healing by promoting neovascularization. While it is commonly agreed that exosomes are the main contributor to stem cell efficacy, further exploration of the effects of EpiSC-EXOs on neovascularization in the context of diabetes could help reveal the potential therapeutic mechanism of EpiSCs.

In vitro, the decreased proliferative and tube formation capabilities under a high-glucose environment are consistent with the findings in the literature. Transcriptome sequencing results showed that differentially expressed genes were mainly enriched in apoptosis and oxidative phosphorylation, which was further validated by Annexin-V/PI and DCFH-DA staining. First, we hypothesized that ROS were the main cause of apoptosis of HUVECs in a high-glucose environment, while the use of the ROS scavenger NAC had no effect on the apoptosis rate of HUVECs in a high-glucose environment. Therefore, ROS may be just artifacts rather than factors that leads to apoptosis.

It is widely accepted that a persistent high-glucose environment leads to metabolic stress, endoplasmic reticulum stress, protein unfolding reactions and mitochondrial damage. All these abnormalities lead to the accumulation of ROS and erroneous metabolites as well as organelle damage, ultimately leading to a decrease in cell viability in a high-glucose environment. We also observed the up regulation of ER stress related genes and decreased Mitochondrial membrane potential in high glucose treated HUVECs, demonstrating that these biological processes may be factors leading to apoptosis. In response to various negative aspects of a high-glucose environment, autophagy is induced as an intracellular self-cleaning mechanism to remove abnormal metabolites or impaired organelles. Autophagy and apoptosis are in a state of dynamic equilibrium. Upregulation of autophagy by appropriate external stimuli helps to remove impurities that accumulate and further promote cell survival, while excessive autophagy induced by excessive external stimuli leads to autophagy-induced apoptosis. In our study, we found that a high-glucose environment causes excessive autophagy, further leading to apoptosis, suggesting that autophagy is the main cause of apoptosis in a high-glucose environment.

Constituting one of the most important components in exosomes, miRNAs function as posttranscriptional regulators to further modulate biological processes within cells. We sequenced differentially expressed miRNAs in EpiSC-EXOs and FB-EXOs and found that miR200b-3p had a significant effect on the apoptosis of vascular endothelial cells in a high-glucose environment. To investigate how miR200b-3p affects apoptosis, a sequencing comparison was used to identify target genes. The results revealed 7 genes as potential targets of miR200b-3p, among which SYDE1 was the most downregulated gene. Consistent with the literature and our previous speculation, SYDE1 functions as a negative regulator of RAS and further influences the MAPK pathway and autophagy, which explains the effect of miR200b-3p on the apoptosis of HUVECs in a high-glucose environment. At the same time, we found that miR200b-3p affected the level of ROS and ER stress (Fig. S3C), and we speculate that this phenomenon may be related to the impact of miR200b-3p on other biological processes. We also noted that, as potential miR200b-3p targets, the other 6 genes have been reported to be significantly related to diabetic complications in epidemiological screening. Nonetheless, it remains unknown whether miR200b-3p has an effect on other biological processes to improve cell survival.

Conclusions

In summary, our study showed that Epidermal stem cells (EpiSCs) could promote angiogenesis and accelerate wound healing in diabetic mice. We also found that high-glucose environment induced the up regulation of reactive oxygen species (ROS) and excessive autophagy, while excessive autophagy, not ROS, is the main cause of apoptosis in HUVECs. miR200b-3p, whose abundance increased in EpiSC-EXOs, could reduce apoptosis in a high-glucose environment through the SYDE1/RAS/ERK/autophagy pathway. Our study provides a theoretical basis for EpiSC effectiveness and suggests the safety of EpiSCs in treating diabetic wounds. The mechanism of the effect of EpiSC-EXOs on wound healing warrants further study to understand the therapeutic effects of EpiSCs and expand their therapeutic scope for diseases.

Abbreviations

EpiSC: Epidermal stem cell

EpiSC-EXO: Epidermal stem cell derived exosome

FB-EXO: Fibroblast derived exosome

ROS: reactive oxygen species

HUVEC: Human Umbilical Vein Endothelial Cells

SYDE1: Synapse Defective Rho GTPase Homolog 1

Declarations

Ethics approval and consent to participate

This study is approved by ICE for Clinical Research and Animal Trials for the First Affiliated Hospital of Sun Yat-sen University. Approval No: [2022]238

Consent for publication

Not applicable

Availability of data and materials

The datasets used and/or analysed during the current study are available from the corresponding author on reasonable request.

Competing interests

The authors declare that they have no conflicts of interest

Funding

This work was supported in part by the National Natural Science Foundation of China (82172949, 81972569, 91772925, 82072180), and the Sun Yat-sen University Clinical Research 5010 Program (2018003)

Authors' contributions

Hailin Xu: Methodology, Validation, Writing – original draft. **Zhiyong Wang:** Methodology , Writing – review & editing. **Hao Yang:** Methodology, Visualization, Data curation. **Chufen Chen, Dongming Lv:** Methodology, Software. **Mingzhou Yuan, Xiaoyan Wang:** Investigation. **Yunxian Dong, Miao Chen, Bing Tang:** Writing –revising. **Peng Wang, Zhongye Xu:** data suggestion. **Zhicheng Hu, Wuguo Deng, Jiayuan Zhu:** Conceptualization, Supervision, Project administration.

Acknowledgements

The present work is the result of all joint efforts. We wish to express our sincere appreciation to all those who have offered the invaluable help during this study. The author gratefully acknowledge the support of Shanhui Ge, who provide valuable assistance with the laboratory suggestion and accompany during this study.

Authors' information (optional)Conflicts of Interest

Not applicable

References

1. Sun H, Saeedi P, Karuranga S, Pinkepank M, Ogurtsova K, Duncan BB, et al. IDF Diabetes Atlas: Global, regional and country-level diabetes prevalence estimates for 2021 and projections for 2045. Diabetes Res Clin Pract. 2022;183:109119.
2. Dixon D, Edmonds M. Managing Diabetic Foot Ulcers: Pharmacotherapy for Wound Healing. Drugs. 2021;81(1):29–56.
3. Schaper NC, van Netten JJ, Apelqvist J, Bus SA, Hinchliffe RJ, Lipsky BA. Practical Guidelines on the prevention and management of diabetic foot disease (IWGDF 2019 update). Diab/Metab Res Rev. 2020;36(Suppl 1):e3266.
4. Okonkwo UA, DiPietro LA. Diabetes and Wound Angiogenesis. International journal of molecular sciences. 2017;18(7).
5. Patel S, Srivastava S, Singh MR, Singh D. Mechanistic insight into diabetic wounds: Pathogenesis, molecular targets and treatment strategies to pace wound healing. 112: Biomedicine & pharmacotherapy = Biomedecine & pharmacotherapie; 2019. p. 108615.
6. Veith AP, Henderson K, Spencer A, Sligar AD, Baker AB. Therapeutic strategies for enhancing angiogenesis in wound healing. Adv Drug Deliv Rev. 2019;146:97–125.
7. Kaushik K, Das A. Endothelial progenitor cell therapy for chronic wound tissue regeneration. Cytotherapy. 2019;21(11):1137–50.
8. Chang M, Nguyen TT. Strategy for Treatment of Infected Diabetic Foot Ulcers. Acc Chem Res. 2021;54(5):1080–93.
9. Huang X, Liang P, Jiang B, Zhang P, Yu W, Duan M, et al. Hyperbaric oxygen potentiates diabetic wound healing by promoting fibroblast cell proliferation and endothelial cell angiogenesis. Life Sci. 2020;259:118246.
10. Zarei F, Negahdari B, Eatemadi A. Diabetic ulcer regeneration: stem cells, biomaterials, growth factors. Artificial cells, nanomedicine, and biotechnology. 2018;46(1):26–32.
11. Hu ZC, Chen D, Guo D, Liang YY, Zhang J, Zhu JY, et al. Randomized clinical trial of autologous skin cell suspension combined with skin grafting for chronic wounds. Br J Surg. 2015;102(2):e117-23.
12. Hu Z, Guo D, Liu P, Cao X, Li S, Zhu J, et al. Randomized clinical trial of autologous skin cell suspension for accelerating re-epithelialization of split-thickness donor sites. Br J Surg. 2017;104(7):836–42.
13. Huang S, Hu Z, Wang P, Zhang Y, Cao X, Dong Y, et al. Rat epidermal stem cells promote the angiogenesis of full-thickness wounds. Stem Cell Res Ther. 2020;11(1):344.
14. Wang P, Hu Z, Cao X, Huang S, Dong Y, Cheng P, et al. Fibronectin precoating wound bed enhances the therapeutic effects of autologous epidermal basal cell suspension for full-thickness wounds by improving epidermal stem cells' utilization. Stem Cell Res Ther. 2019;10(1):154.
15. Doyle LM, Wang MZ. Overview of Extracellular Vesicles, Their Origin, Composition, Purpose, and Methods for Exosome Isolation and Analysis. Cells. 2019;8(7).

16. Kalluri R, LeBleu VS. The biology, function, and biomedical applications of exosomes. Science (New York, NY). 2020;367(6478).
17. Li X, Xie X, Lian W, Shi R, Han S, Zhang H, et al. Exosomes from adipose-derived stem cells overexpressing Nrf2 accelerate cutaneous wound healing by promoting vascularization in a diabetic foot ulcer rat model. Exp Mol Med. 2018;50(4):1–14.
18. Lopes L, Setia O, Aurshina A, Liu S, Hu H, Isaji T, et al. Stem cell therapy for diabetic foot ulcers: a review of preclinical and clinical research. Stem Cell Res Ther. 2018;9(1):188.
19. Wang P, Theocharidis G, Vlachos IS, Kounas K, Lobao A, Shu B, et al. Exosomes Derived from Epidermal Stem Cells Improve Diabetic Wound Healing. The Journal of investigative dermatology; 2022.
20. Pegtel DM, Gould SJ. Exosomes. Annu Rev Biochem. 2019;88:487–514.
21. Lu TX, Rothenberg ME. MicroRNA. J Allergy Clin Immunol. 2018;141(4):1202–7.
22. Bushati N, Cohen SM. microRNA functions. Annual review of cell and developmental biology. 2007;23:175–205.
23. Mohr AM, Mott JL. Overview of microRNA biology. Semin Liver Dis. 2015;35(1):3–11.
24. Zhang J, Li S, Li L, Li M, Guo C, Yao J, et al. Exosome and exosomal microRNA: trafficking, sorting, and function. Genom Proteom Bioinform. 2015;13(1):17–24.
25. Maiuri MC, Zalckvar E, Kimchi A, Kroemer G. Self-eating and self-killing: crosstalk between autophagy and apoptosis. Nat Rev Mol Cell Biol. 2007;8(9):741–52.
26. Doherty J, Baehrecke EH. Life, death and autophagy. Nat Cell Biol. 2018;20(10):1110–7.
27. Thorburn A. Crosstalk between autophagy and apoptosis: Mechanisms and therapeutic implications. Prog Mol Biol Transl Sci. 2020;172:55–65.
28. Kaminskyy VO, Zhivotovsky B. Free radicals in cross talk between autophagy and apoptosis. Antioxid Redox Signal. 2014;21(1):86–102.
29. Fernández A, Ordóñez R, Reiter RJ, González-Gallego J, Mauriz JL. Melatonin and endoplasmic reticulum stress: relation to autophagy and apoptosis. J Pineal Res. 2015;59(3):292–307.
30. Glick D, Barth S, Macleod KF. Autophagy: cellular and molecular mechanisms. J Pathol. 2010;221(1):3–12.
31. Wang Y, Xiong H, Liu D, Hill C, Ertay A, Li J, et al. Autophagy inhibition specifically promotes epithelial-mesenchymal transition and invasion in RAS-mutated cancer cells. Autophagy. 2019;15(5):886–99.
32. Zhao X, Su L, He X, Zhao B, Miao J. Long noncoding RNA CA7-4 promotes autophagy and apoptosis via sponging MIR877-3P and MIR5680 in high glucose-induced vascular endothelial cells. Autophagy. 2020;16(1):70–85.
33. Lo HF, Tsai CY, Chen CP, Wang LJ, Lee YS, Chen CY, et al. Association of dysfunctional synapse defective 1 (SYDE1) with restricted fetal growth - SYDE1 regulates placental cell migration and invasion. J Pathol. 2017;241(3):324–36.

Figures

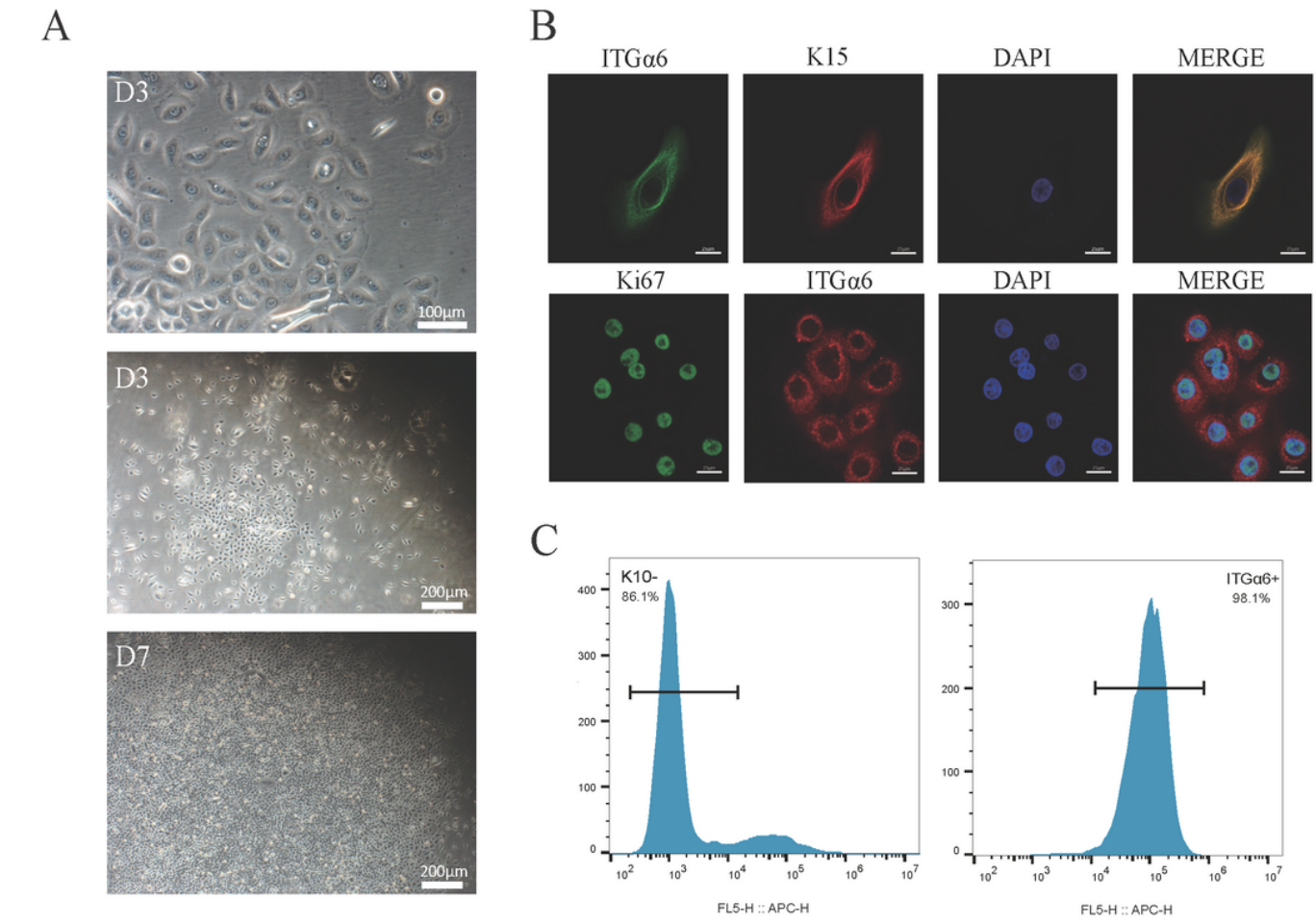

Figure 1

Identification of EpiSCs. A) Human EpiSC morphology on the 3rd and 7th days. B) Identification of third-generation cells via Ki67, ITGα6, and Ck15. C) Flow cytometry to detect the proportion of K10-negative and ITGα6-positive cells.

FIG.2

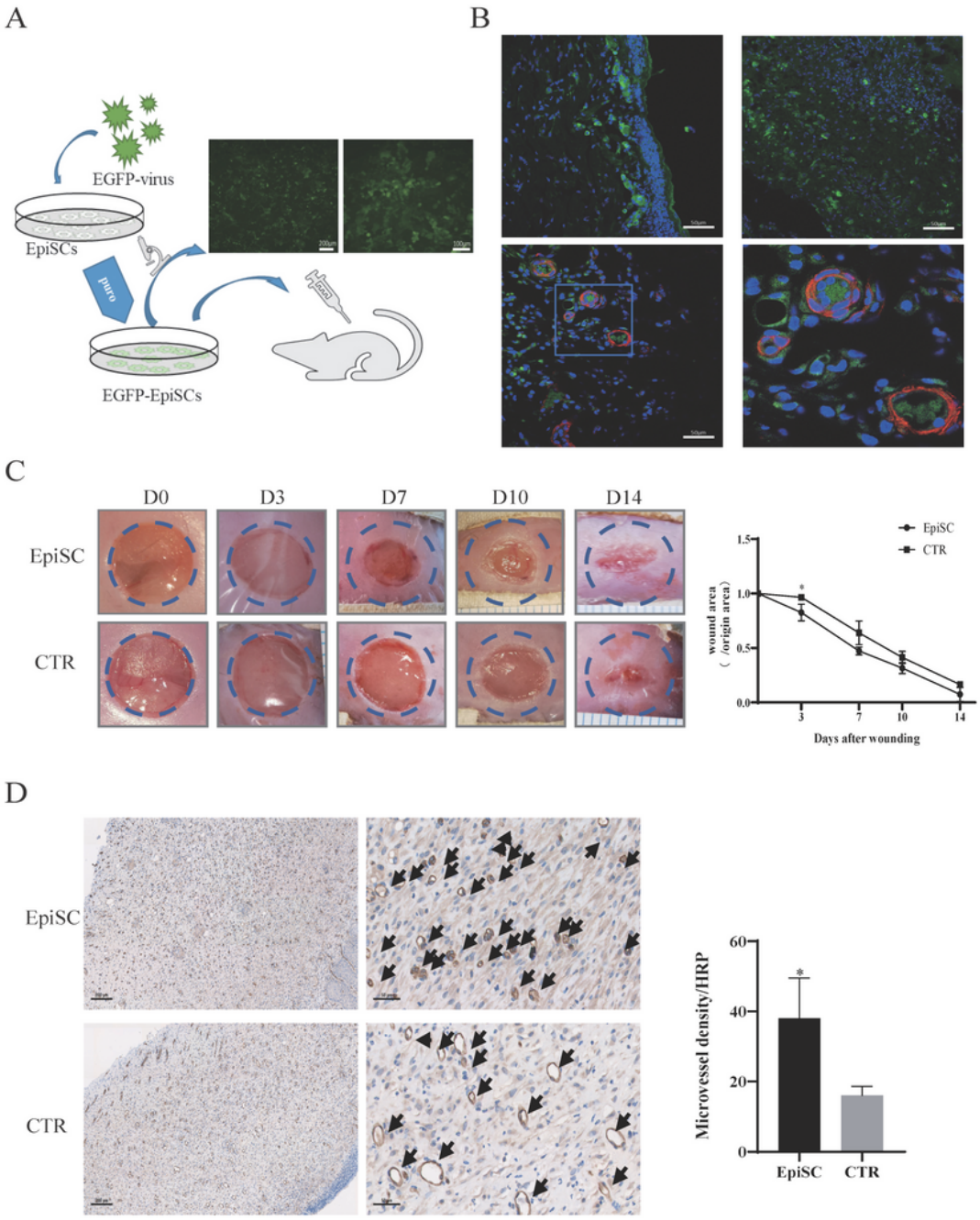

Figure 2

EpiSCs can proliferate and accelerate wound healing by promoting angiogenesis. A) Mice EpiSCs were transfected with lentivirus to stably express EGFP. B) Representative area of wound tissue sections stained with α-SMA on postinjury day 7 showing EpiSCs colonizing the wound area and surrounding microvasculature in mouse wounds in the EpiSC group. C) Images of wounds on the dorsal skin of mice in the negative control group and EpiSC group were taken on postinjury days 0, 3, 7, 10, and 14. D)

Representative area and analysis of wound tissue sections stained with CD31 on postinjury day 7 showing microvascular regeneration in mouse wounds in the negative control group and ESC group. The arrows indicate the microvasculature. *, P <0.05; **, P <0.01; ***, P <0.001.

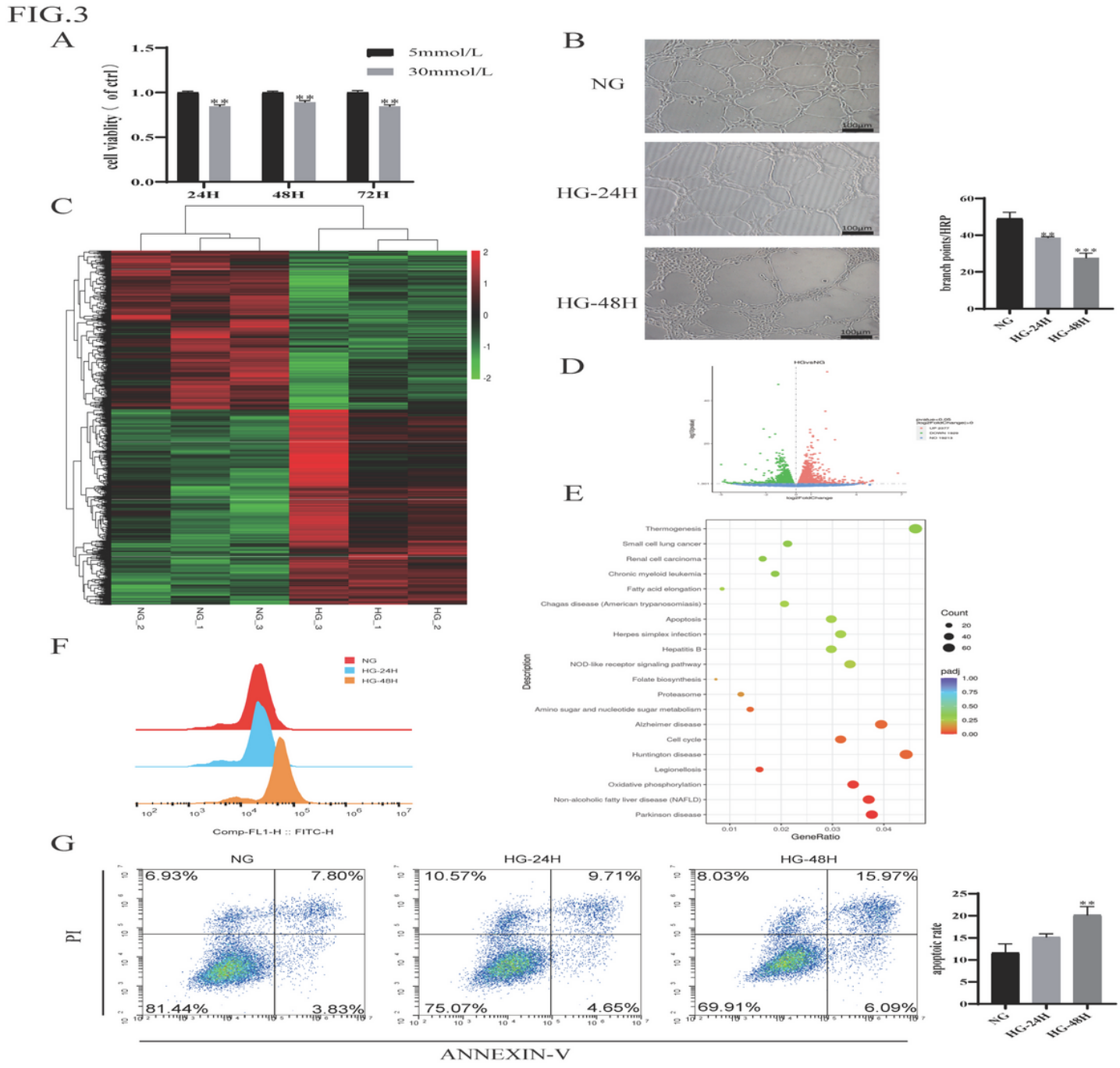

Figure 3

High glucose induces the dysfunction and apoptosis of HUVECs. A) CCK-8 assays showing a decrease in the proliferation of HUVECs under different concentrations and durations of glucose treatment. B) Representative images of the tube formation ability of HUVECs under high glucose for different treatment times. C) Differential gene cluster analysis of HUVECs under different concentrations of glucose. D) Volcano plot of differentially expressed genes. E) Bubble map of the pathway enrichment analysis. F)

Flow cytometry analysis of intracellular ROS levels in HUVECs subjected to different concentrations of glucose. G) Flow cytometry analysis of the apoptosis rate of HUVECs under different concentrations of glucose. *, P <0.05; **, P <0.01; ***, P <0.001.

FIG.4

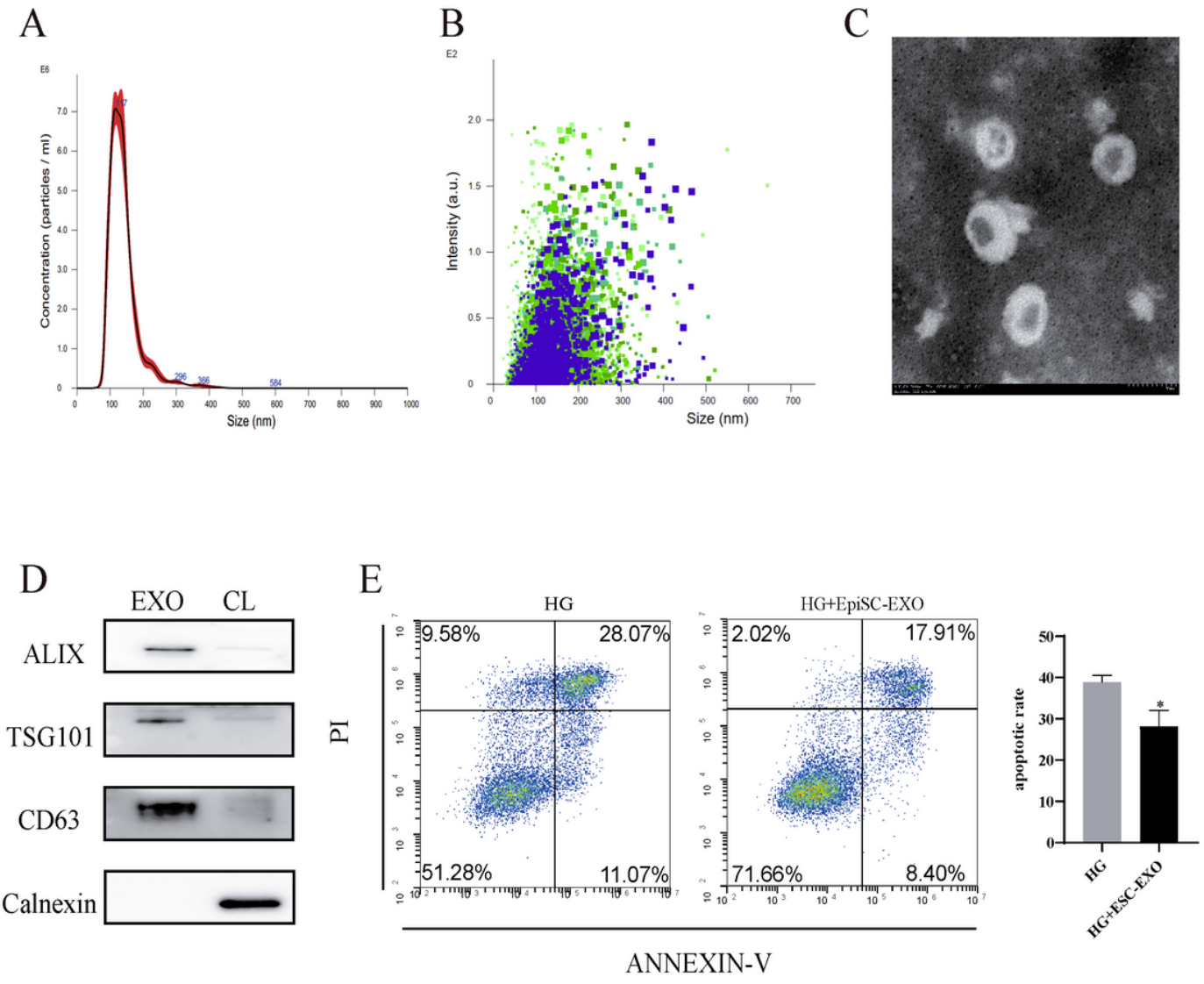

Figure 4

EpiSC-EXOs alleviate the apoptosis of HUVECs under high glucose. A, B) Exosome size distribution examined through NTA. C) Representative electron microscopy image of EpiSC-EXOs. D) Exosome-associated proteins were validated with western blotting. E) Flow cytometry analysis of the apoptosis rate of HUVECs treated with EpiSC-EXOs. *, P <0.05; **, P <0.01; ***, P <0.001.

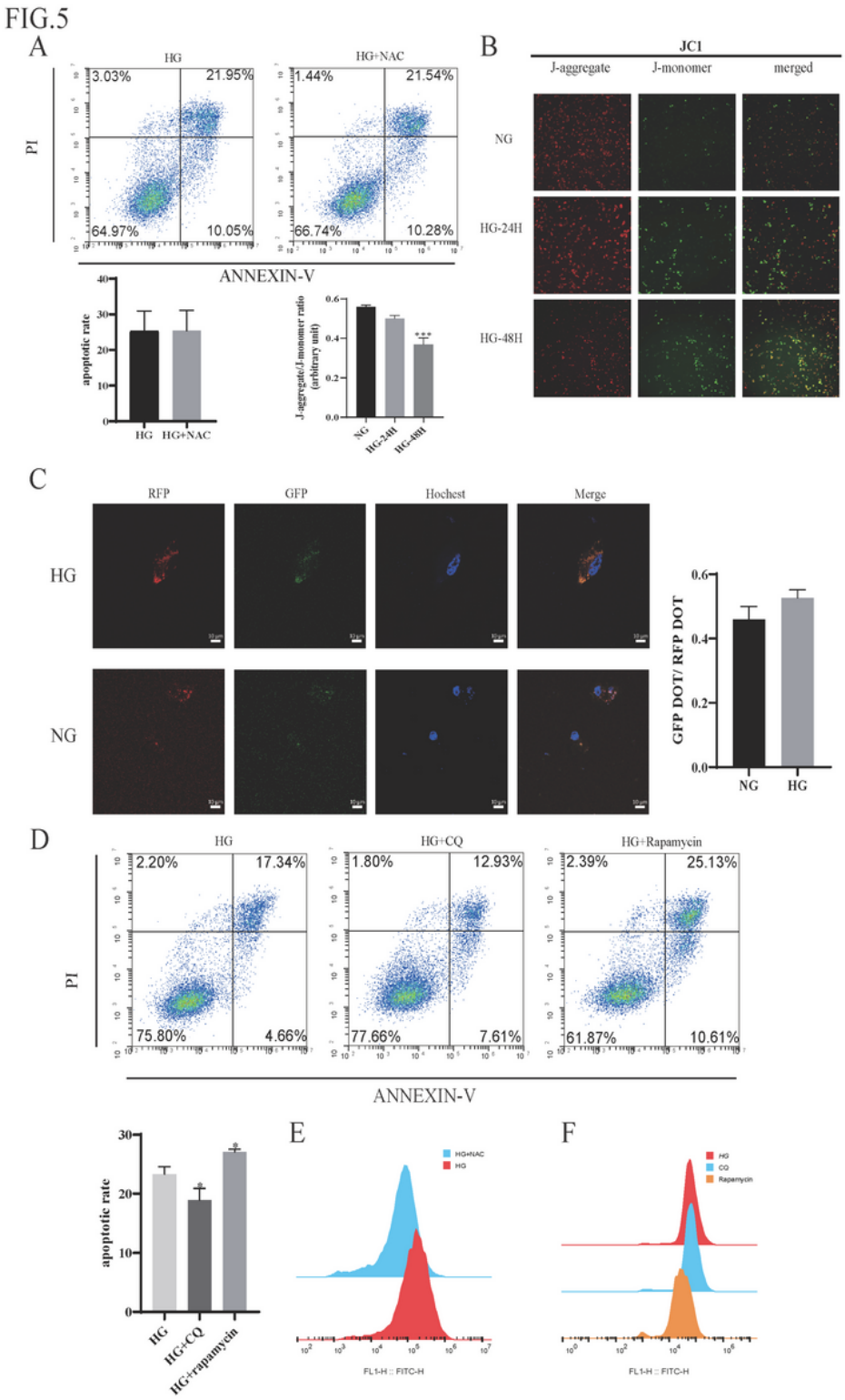

Figure 5

Autophagy decreases ROS and promotes apoptosis induced by high-glucose conditions. A) Flow cytometry analysis of the apoptosis rate of HUVECs treated with NAC. B) Representative image and analysis of mitochondrial membrane potential. JC-1 stains mitochondria with a strong membrane potential red and mitochondria with a weak membrane potential green. C) Representative mRFP-eGFP-LC3 fluorescence picture of HUVECs under different concentrations of glucose. D) Flow cytometry

analysis of the apoptosis rate of HUVECs treated with rapamycin and CQ. E) Flow cytometry analysis of intracellular ROS levels in HUVECs treated with NAC. F) Flow cytometry analysis of intracellular ROS levels in HUVECs treated with rapamycin and CQ. *, P <0.05; **, P <0.01; ***, P <0.001

FIG.6

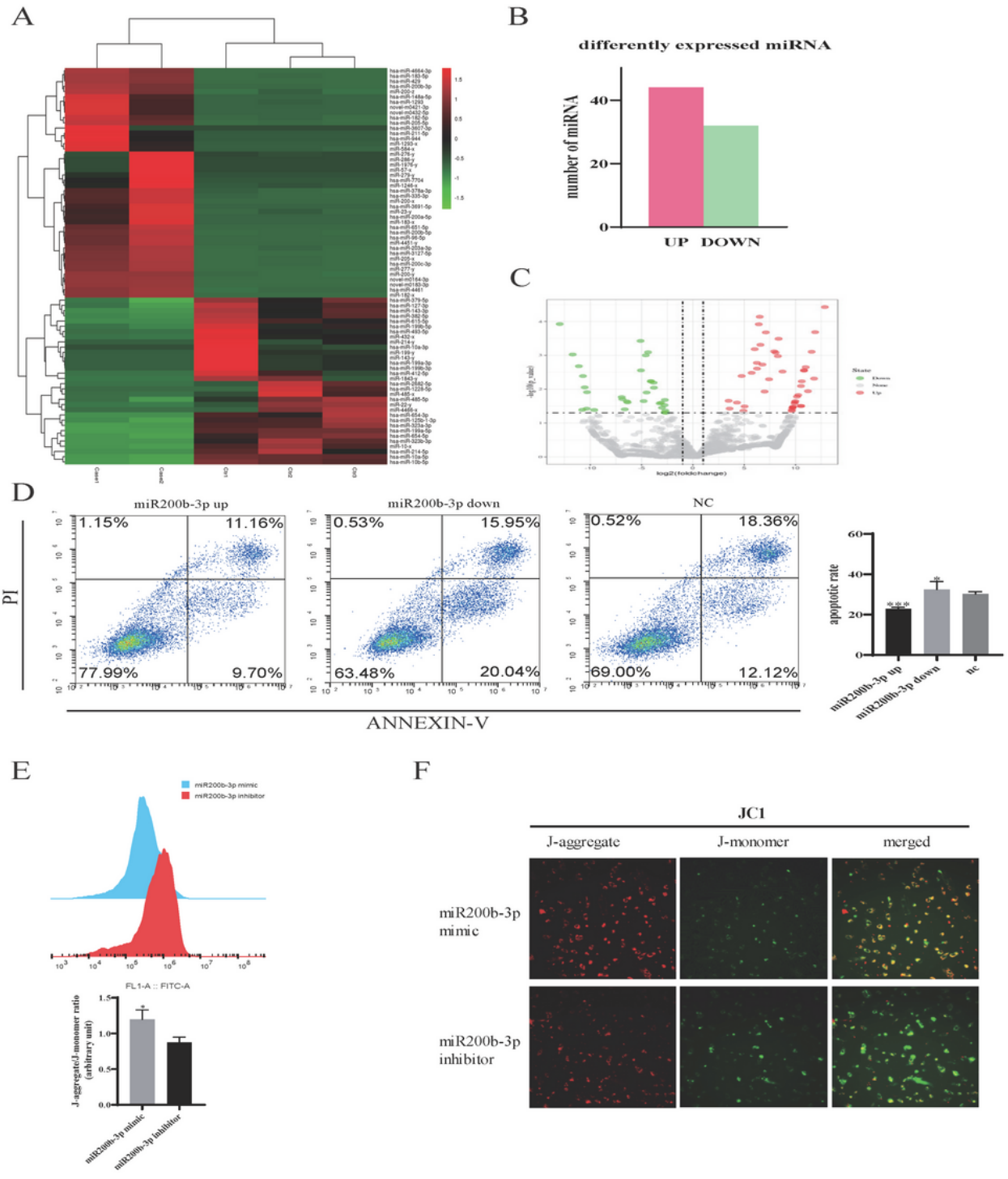

Figure 6

EpiSC-EXOs alleviate the apoptosis of HUVECs in a high-glucose environment by the delivery of miR200b-3p. A) Differential miRNA cluster analysis of EpiSC-EXOs and FB-EXOs. B) Differential miRNAs in EpiSC-EXOs and FB-EXOs. C) Volcano plot of differentially expressed miRNAs in EpiSC-EXOs and FB-EXOs. D) Flow cytometry analysis of the apoptosis rate of HUVECs overexpressing miR200b-3p (miR200b-3p up) and knocking down miR200b-3p (miR200b-3p down) and the negative control (NC). E) Flow cytometry analysis of the intracellular ROS levels of HUVECs differentially expressing miR200b-3p. F) Representative image and analysis of the mitochondrial membrane potential of HUVECs differentially expressing miR200b-3p. *, P <0.05; **, P <0.01; ***, P <0.001

FIG.7

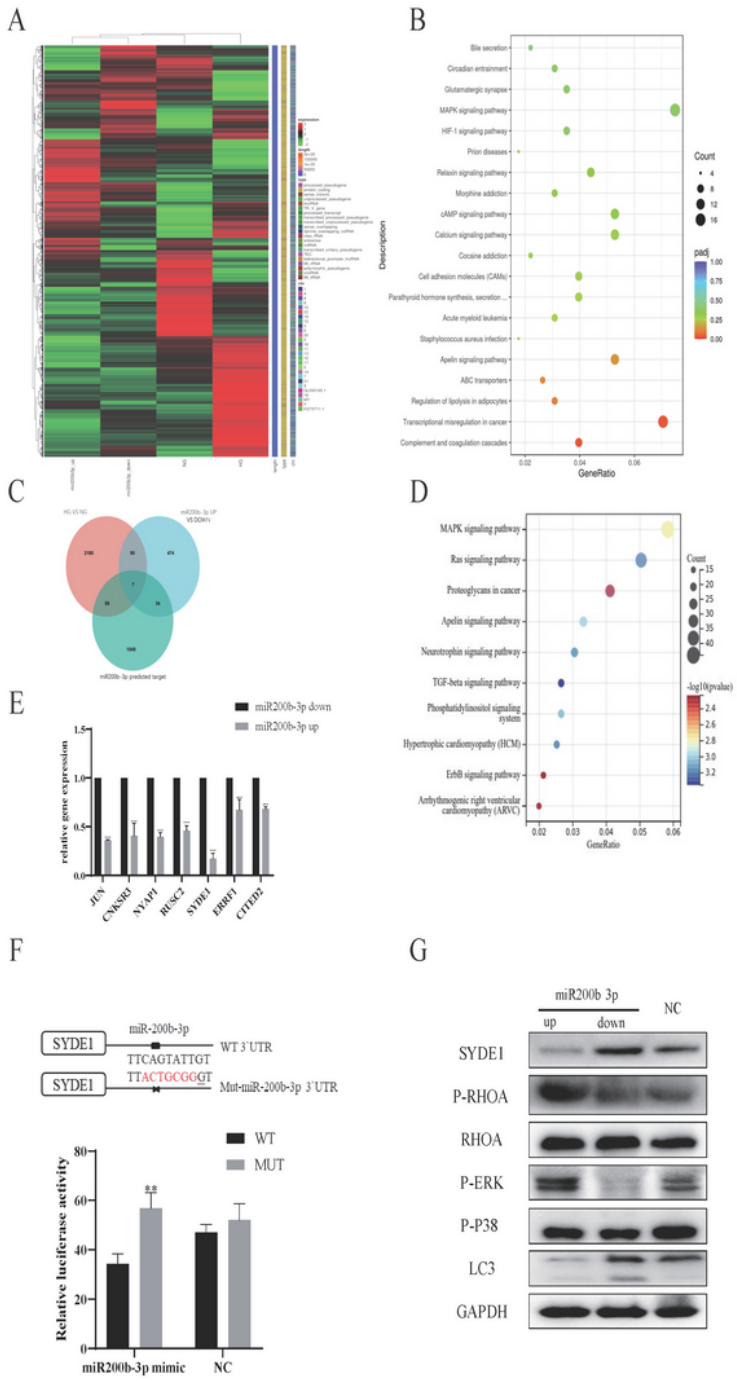

Figure 7

miR200b-3p-mediated upregulation of the MAPK pathway decreases autophagy through downregulation of SYDE1. A) Differential gene cluster analysis of HUVECs overexpressing miR200b-3p (miR200b-3p up) and knocking down miR200b-3p (miR200b-3p down) and treated with different concentrations of glucose. B) Bubble map of the pathway enrichment analysis of HUVECs differentially expressing miR200b-3p. C) Intersection of the differentially expressed genes of HUVECs differentially expressing

miR200b-3p treated with different concentrations of glucose and miR200b-3p predicted targets. D) Bubble map of the pathway enrichment analysis of miR200b-3p predicted target. E) qPCR of 7 miR200b-3p predicted target genes in HUVECs differentially expressed miR200b-3p and negative control. F) Dual-luciferase reporter gene assay showing that SYDE1 is a target of miR200b-3p. G) Western blot of SYDE1, P-RHOA, RHOA, P-ERK, P-38, LC3, and GAPDH expression in HUVECs differentially expressing miR200b-3p and the negative control. *, P <0.05; **, P <0.01; *** P <0.001

FIG.8

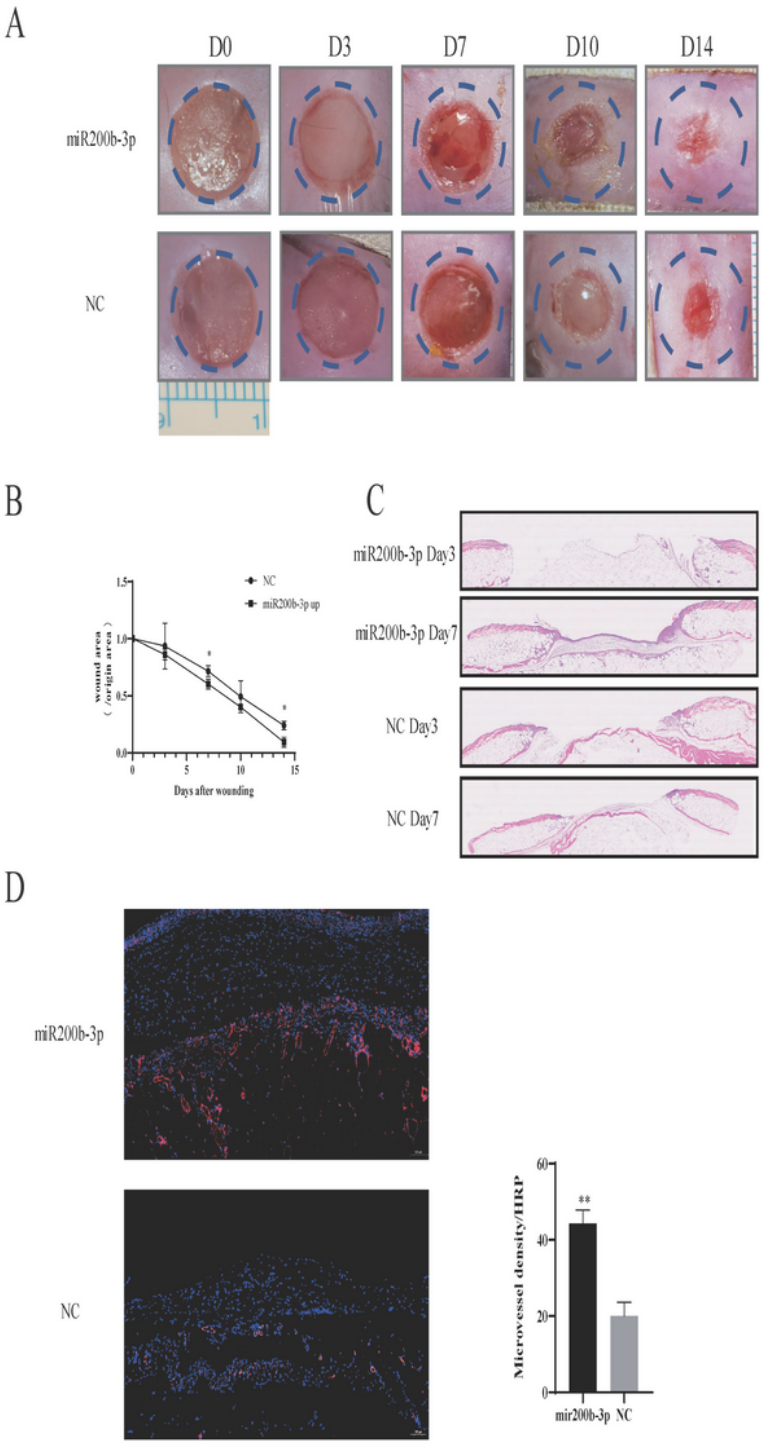

Figure 8

miR200b-3p accelerates wound healing by promoting angiogenesis in diabetic mice. A) Images of wounds on the dorsal skin of mice in the miR200b-3p group and negative control (NC) group taken on postinjury days 0, 3, 7, 10, and 14. B) Residual wound rates of the miR200b-3p group and negative control (NC) group on postinjury days 0, 3, 7, and 14. C) Representative HE image of wound tissue sections in the miR200b-3p group and negative control (NC) group. D) Representative area and analysis of wound tissue sections stained with CD31 on postinjury days 7 and 14, showing microvascular regeneration in mouse wounds in the miR200b-3p group and negative control (NC) group.

Supplementary Files

This is a list of supplementary files associated with this preprint. Click to download.

- graphicalabstract.pdf
- supplementdata2.0.pdf